

MONTE CARLO ANALYSIS OF ENCIRCLED AND ENSQUARED ENERGY  
VARIABILITY  
WITH RMS WAVEFRONT ERROR

by

Sze Wah Lee

---

Copyright © Sze Wah Lee 2023

A Thesis Submitted to the Faculty of the

JAMES C. WYANT COLLEGE OF OPTICAL SCIENCES

In Partial Fulfillment of the Requirements

For the Degree of

MASTER OF SCIENCE

In the Graduate College

THE UNIVERSITY OF ARIZONA

2023

THE UNIVERSITY OF ARIZONA  
GRADUATE COLLEGE

As members of the Master's Committee, we certify that we have read the thesis prepared by **Sze Wah Lee**, titled **Monte Carlo Analysis of Encircled and Ensquared Energy Variability with RMS Wavefront Error** and recommend that it be accepted as fulfilling the thesis requirement for the Master's Degree.

*Jose Sasián*  
\_\_\_\_\_  
Professor José M. Sasián

Date: 08/14/2023

*Rongguang Liang*  
\_\_\_\_\_  
Professor Rongguang Liang

Date: 08/14/2023

*Ronald G. Driggers*  
\_\_\_\_\_  
Professor Ronald G. Driggers

Date: 08/14/2023

Final approval and acceptance of this thesis is contingent upon the candidate's submission of the final copies of the thesis to the Graduate College.

I hereby certify that I have read this thesis prepared under my direction and recommend that it be accepted as fulfilling the Master's requirement.

*Jose Sasián*  
\_\_\_\_\_  
Professor José M. Sasián  
Master's Thesis Committee Chair  
Wyant College of Optical Sciences

Date: 08/14/2023

ARIZONA

## Acknowledgements

I would like to thank:

Dr. Jose Sasian, for guiding me and encouraging me to keep going with my work.

Dennis Douglas for providing previous work done on the simulation.

Robert Murphy, for being my first mentor at my first job. Thank you being kind and patient, and mostly, building the optical engineer I am today.

My parents, who gave up their life in Hong Kong so I can have more opportunities to find who I want to be in America. Thank you for believing in me.

My sister, brother, friends, and loved ones. Thank you for the unconditional love and support.

Lastly, an honorable mention, my cat Mooshu, for sitting through all my Zoom lectures with me.

# Contents

List of Figures .....	5
List of Tables .....	6
Abstract .....	7
Introduction.....	8
Section 1: Background.....	13
1.1 Impulse Response and Optical Transfer Function .....	13
1.2 Wavefront Aberrations.....	15
1.3 Encircled and Ensquared Energy General Application.....	19
1.3.1 Ensquared and Ensquared Measurement Methods .....	20
1.3.2 Encircled and Ensquared Energy Analytical Solution Comparison.....	22
Section 2: Simulation.....	25
2.1 Simulation Scope and Parameters.....	25
2.2 Monte Carlo Zemax Set Up .....	26
Section 3: Results.....	28
3.1 Plots of Raw data .....	29
3.1.1 Zernike .....	29
3.2.2 F-Number .....	31
3.2.3 Wavelength .....	32
3.2 Fitted Equations .....	33
Section 4: Discussion.....	36
Section 5: Conclusion .....	38
Appendix 1.....	40
Zemax Macro .....	40
Matlab Code.....	42
References.....	43

## List of Figures

Figure 1: An obscured aperture defined by constant transmission region, $g$ , and zero transmission as $g'$ . The resultant geometry is used for autocorrelating the transmission region in the direction of $a$ . (1).....	9
Figure 2: MTF Plot of a Diffraction Limited System: F/1.48 at 1 $\mu\text{m}$ .....	14
Figure 3: The normalized pupil coordinate is composed of radial distance on a pupil plane, $\rho$ , and angular circular component, $\theta$ .....	16
Figure 4 :Inscribe energy region centered on the PSF. Left Encircled. Right Ensquared. [3].....	19
Figure 5 Test Bench to measure Encircled Energy.....	20
Figure 6:Cross section of the Point Spread Function of a F/1.4 system at 1 $\mu\text{m}$ in color scale. ....	21
Figure 7: Cross section of the PSF with various rms wavefront error. ....	21
Figure 8 : Fractional inscribe energy of a diffraction limited F/1.4 system at 1 $\mu\text{m}$ . Ensquared Energy curve is slightly higher than the Encircled energy because circle is inscribed within the square of the same width. More area per the same width dimension. ....	22
Figure 9 Radial distance of Ensquared Energy, $p$ . ....	23
Figure 10 Simulation Zemax Lens Data Manager .....	26
Figure 11: Example Output File of Zemax Simulation.....	28
Figure 12: Zernike Order: 4th,5th, 4th + 5 <sup>th</sup> and All Order (2 <sup>nd</sup> to 5 <sup>th</sup> Order) WFE vs Encircled and Ensquared Energy Radius. ....	30
Figure 13 F-number with Zernike WFE vs Encircled and Ensquared Energy Radius.....	31
Figure 14 Wavelength with Zernike WFE vs Encircled and Ensquared Energy Radius. ....	32
Figure 15: Secondary Coma (6) .....	37

## List of Tables

Table 1: All different orders of Zernike's expression and corresponding aberration name. (5).....	17
Table 2: Three different sample sizes were analyzed for each targeted wavefront error.....	27
Table 3: 85% Encircled and Ensquared energy radius calculated for 2 <sup>nd</sup> to 5 <sup>th</sup> Order Zernike Errors using Equation 51 and 52. ....	35
Table 4: 83.8% Encircled Energy radius calculated for 2 <sup>nd</sup> to 5 <sup>th</sup> Order Zernike Errors using Equation 53 .....	35
Table 5: Comparison of Analytical Solution vs Monte Carlo Results from 85% and 85% Inscribe Energy. .....	36

## Abstract

Analytical calculations for encircled and ensquared energy have limitations. When aberrations are present, analytical methods are often intractable. Modelling and simulation can be an alternative approach. A Monte Carlo analysis is performed to generate unique combinations of Zernike wavefront errors that yield the same overall rms error of the optical system. Zernike errors from orders 2<sup>nd</sup> through 5<sup>th</sup> are considered individually, as well as errors from 4<sup>th</sup> and 5<sup>th</sup> orders combined. Finally, all orders from 2<sup>nd</sup> to 5<sup>th</sup> are considered in combination. The optical systems simulated are f/1.4, f/4, f/6, and f/8 at operating wavelengths of 0.633  $\mu\text{m}$ , 1  $\mu\text{m}$  and 3.39  $\mu\text{m}$ . Relationships between the encircled and ensquared energy radius are determined for rms wavefront error  $< 0.18$  waves. The most realistic relationship derived is for the case of 2<sup>nd</sup> to 5<sup>th</sup> Order Zernike considered in combination. Given a known rms wavefront error ( $wfe$ ) in unit of waves, the approximated 85% encircled energy radius is  $1.50 \lambda f/\# e^{\frac{5.21 wfe}{\lambda}}$ , and ensquared energy radius is  $1.31 \lambda f/\# e^{\frac{5.53 wfe}{\lambda}}$ . The Monte Carlo derived trendlines match the simulated aberrated systems to within a residual sum of squares, RSS, error of 5%. An additional equation is derived for simplification purposes with slightly higher RSS error. The approximated 83.8% Encircled energy radius is  $1.22 \lambda f/\# e^{\frac{2\pi wfe}{\lambda}}$  with RSS fitting error of 10%.

## Introduction

There are various published papers deriving analytical methods to solve for encircled energy of an optical system. Although this thesis work is done on optical software simulation, it is important to understand the analytical solution space as well as its limitations.

From a 1984 a paper published in Applied Optics (1), the following formulas are derived. At the image plane, the point spread function (PSF) is the inverse Fourier transform of the optical transfer function (OTF). The relationship can be written as the following:

$$I(r, \theta) = K_1 \int_0^{2\pi} \int_0^\infty T(\rho, \varphi) e^{\left(\frac{ikr\rho}{f} \cos(\varphi - \theta)\right)} \rho d\rho d\varphi \quad [1]$$

$I(r, \theta) =$  Point Spread Function (PSF),

$(r, \theta) =$  polar coordinate in the image plane,

$T(\rho, \varphi) =$  OTF,  $(\rho, \varphi) =$  polar coordinates in entrance pupil,  $k = \frac{2\pi}{\lambda}$ ,

$\lambda =$  wavelength,  $f =$  effective focal length, and  $K_1 =$  constant.

The encircled energy is then the integration of the PSF over a radius  $r_o$

$$E(r_o) = \int_0^{2\pi} \int_0^{r_o} I(r, \theta) r dr d\theta \quad [2]$$

A new function is defined  $\bar{T}(\rho)$  as the average of  $T(\rho, \varphi)$  over all angles of  $\varphi$ .

$$\bar{T}(\rho) = \frac{4\pi^2 K_1 f r_o}{k} \int_0^{2\pi} T(\rho, \varphi) d\varphi \quad [3]$$

The encircled energy function for any size aperture then becomes the following integral...

$$E(r_o) = \frac{4\pi^2 f^2 K_1}{k^2} \int_0^\infty \bar{T}(\rho) J_1\left(\frac{kr_o\rho}{f}\right) d\rho \quad [4]$$

Using Taylor series expansion, Equation [4] is then expanded in the following format.

$$E(r_o) = \frac{4\pi^2 f^2 K_1}{k^2} \left[ \bar{T}(0) + \frac{f}{kr_o} \bar{T}'(0) + \frac{f^3}{2k^3 r_o^3} \bar{T}'''(0) + \dots \right] \quad [5]$$

Note that the OTF function derived from a finite boundary geometry will not have analytical solutions beyond some cut-off frequency. Equation [5] will have convergence issues for smaller

radius,  $r_o$ . If nonanalytical points occurred at  $T(\rho)$  at frequencies below cut off, then Equation [5] will only work for large  $r_o$ . For large  $r_o$ , equation [5] becomes.

$$E(r_o) \sim \frac{4\pi^2 f^2 K_1}{k^2} \left[ \bar{T}(0) + \frac{f}{kr_o} \bar{T}'(0) \right]. \quad [6]$$

Since OTF is unity at zero frequency,  $\bar{T}(0)$  is unity. The normalized encircled energy will be equal to 1 with infinite boundary,

$$\lim_{r_o \rightarrow \infty} E(r_o) = 1 \quad [7]$$

The relationship between the encircled energy function to the derivative of the OTF at zero frequency can be rewritten as [8].

$$E(r_o) \sim 1 + \frac{f}{kr_o} \bar{T}'(0) \quad [8]$$

The derivations above work for unobscured aperture and high frequency OTF. For obscured aperture or low frequency OTF, additional work is needed. Figure 1 describes an obscured entrance pupil of an optical system.

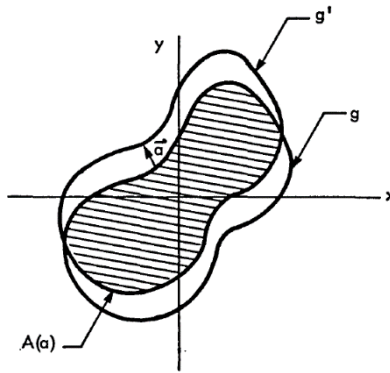


*Figure 1: An obscured aperture defined by constant transmission region,  $g$ , and zero transmission as  $g'$ . The resultant geometry is used for autocorrelating the transmission region in the direction of  $a$ . (1)*

If the original transmission boundary,  $g$ , is displaced along the vector  $a$ , a new boundary  $g'$  is created in Figure 1. The new boundary is described as  $g'(x, y) = g(x - a, y - b)$ . The middle

overlapping area, in crossed pattern in Figure 1, is an obscured aperture used to find an encircled energy solution for. The aperture area,  $A(a)$ , can be described as

$$A(a) = A_0 - \frac{1}{2} \int_0^s |a| |\cos \eta| ds \quad [9]$$

Where  $A(a)$ = overlapping area between  $g$  and  $g'$

$A_0$  = area of  $g(x, y)$

$\eta$ = angle between  $a$  and  $\nabla g$

$s$ =total perimeter length along  $g$

$ds$ =differential arc length along  $g$

In polar coordinates, Equation 9 can be rewritten as

$$A(\rho, \varphi) = A_0 - \frac{1}{2} \int_0^s |\rho| |\cos \eta| ds \quad [10]$$

A new OTF function normalized over the overlapping area between  $g$  and  $g'$  can be written as

$$T(\rho, \varphi) = \frac{A(\rho, \varphi)}{A_0} \quad [11]$$

resulting in a new  $E(r_o)$ ,

$$E(r_o) \sim 1 - \frac{f}{kr_o} \frac{L}{\pi A_0} \quad [12]$$

Where  $L$  is the perimeter length,  $k = \frac{2\pi}{\lambda}$ ,

$A_0$  is the area of the entrance pupil.

This modification works not only for general aperture shapes but also multiple apertures and obscured apertures. For obscured apertures, Equation [10] is replaced by a summation of integrals. Each integral represents one of the sub aperture regions.

For every practical unobscured imaging system, the normalized encircled energy function is asymptotically described as

$$\lim_{r_o \rightarrow \infty} E(r_o) = 1 - \frac{\lambda f R}{2\pi^2 r_o} \quad [13]$$

Where  $E(r_o)$  = encircled energy

$\lambda$  = wavelength

$f$  = effective focal length

$R$  = aperture perimeter to area ratio

$r_o$  = radial dimension in the focal plane

The limitations to using Equation 13 are entrance pupil needs to have constant transmittance, pupil size needs to be larger than the wavelength of interest, and no aberration is present in system. In addition, a careful evaluation of aperture shape with low frequency OTF slope discontinuities is needed. More information on the accuracy and a comparison between the exact and approximate methods can be found in Reference (1).

For optical system with aberrations, Shafer (2) published a paper describing a very similar analytical solution. They first assumed an unobscured optical system with a circular entrance pupil. Then, they revised the OTF to include the effects of aberrations.

Equation [14] below is the series expansion of the transfer function due to defocus,

$$T(\omega) \approx 1 - \frac{2\omega}{\pi} + \frac{\omega^3}{12\pi} - \frac{16}{3}\pi D^2 \left( \frac{3\pi\omega^2}{8} - 2\omega^3 \right) + \dots \quad \text{Higer Order Terms} \quad [14]$$

Where D is the defocus optical path difference in waves, and  $\omega$  is the spatial frequency. (2)

By taking the derivate of the transfer function, the encircled energy equation with defocus is expressed as follows,

$$L(v)_{\text{Perfect System}} \approx 1 - \frac{2}{\pi v} - \frac{1}{4\pi v^3} \quad [15]$$

$$L(v)_{\text{defocus system}} \approx L(v)_{\text{Perfect System}} - \frac{32\pi D^2}{v^3} \quad [16]$$

Where  $L(v)$  = encircled energy  
 $v$  = normalized spot radius  
 $f$  = effective focal length  
 $D$  = Defocus in waves

The normalized spot radius,  $v$ , is dimensionless. Assuming an unobscured circular entrance pupil,  $v$  can be determined using the following Equation [17]

$$v = \frac{r_o \pi d}{f \lambda} \quad [17]$$

$\lambda$  = wavelength  
 $f$  = effective focal length  
 $d$  = diameter of entrance pupil  
 $r_o$  = radial dimension in the focal plane

When substituting in Equation [17] into Equation [15], the new equation for  $L(v)_{Perfect\ System}$  is equivalent to Equation [1] for  $E(r_o)$ . As a verification check, the first and second published paper calculation methods are in agreement.

According to Shafer's method,  $L(v)_{defocus\ system}$ , a system with defocus, will move the energy away from the central lobe into outside rings on the image plane. This is accounted for in an additional subtraction term in Equation [16].  $L(v)_{defocus\ system}$  is most accurate when restricted to a region 80-100% of the size of the total energy size and is limited to aberrations smaller than  $\frac{\lambda}{2}$ . It could also work for any rotationally symmetric wavefront deformation, such as 3<sup>rd</sup> and 5<sup>th</sup> order spherical aberration. However, it is only valid if the marginal ray intercept at the image plane is the same value as the defocus case. In other words, a mirror with spherical aberration will have similar encircled energy value as a mirror with a radius of curvature error if the peak to valley wavefront errors in both cases are the same. However, this will not be the case for a mirror with the same order of magnitude of error with astigmatic deformations. The Encircled Energy value might degrade faster in the case of the mirror with the astigmatic deformation because of the nonrotational symmetric shape. It also varies quadratically with the amount of wavefront error. Therefore, various types of wavefront error cannot be added up linearly.

The two analytical methods discussed shows that Encircled energy is not a straightforward calculation once an optical system deviates from the ideal case of an unobscured circular aperture with no aberrations. Some approximation can be made with rotational symmetric wavefront error but is only valid in cases where the peak to valley error is less than  $\frac{\lambda}{2}$ . In a practical imaging system, there will be unique types of aberration with different magnitude of errors. An alternative approach is introduced in this thesis to create a look up formula for encircled and ensquared values per a given rms wavefront error value.

The thesis will be divided into five sections. The first section is the Background, and it will cover the fundamental of imaging system, wavefront aberrations as well as application and calculation methods of Encircled Energy. The second section, Simulations, will cover the parameters of simulation. The following Results, Discussion and Conclusion sections, will go over the post processing of raw data, establishing the look up formula and conclude on the simulation work.

## Section 1: Background

### 1.1 Impulse Response and Optical Transfer Function

An imaging system is defined by the ability to capture an object at a distance and paste it onto a detector. For a well sampled system, the image is the convolution of the object with the imaging system's impulse response. The impulse response of an optical system is analogous to that from systems' theory, with the usual restrictions of linearity and shift-invariance. For an optical system, a point source is the equivalent input. The imaging system will convert the point source into a point spread function, related through the Fourier transform.

If the optics are perfect, have no aliasing at the detector and have a circular shaped aperture, the PSF is describe by the Equation [18].

$$PSF(r) = \left( \frac{2J_1 \frac{\pi dr}{\lambda f}}{\frac{\pi dr}{\lambda f}} \right)^2 \quad [18]$$

Where  $r$  = radial distance on the image,  
 $\lambda$  = wavelength,  $f$  = effective focal length,  
and  $d$  = diameter of entrance pupil.

This is also known as the airy disk. The central lobe contains ~84% of the total energy on the image plane. The radius of the same bright central lobe is

$$r_1 = \frac{1.22\lambda f}{d} \quad [19]$$

In summary, the impulse function is the way an optical system interprets spatially how big or small the image is. The three parameters that affects the spatial interpretations are wavelength ( $\lambda$ ), focal length( $f$ ) and aperture size ( $d$ ).

The object frequency information is calculated by taking the Fourier transform of the input irradiance. This value information is then multiplied with a transfer function, known as OTF, of the imaging system to yields the output frequency information. The inverse Fourier transform of the output frequency information is the image in spatial domain. Similarly, the OTF is the Fourier transform of the impulse response. The OTF has both magnitude and phase. The modulus of the squared magnitude of the OTF is called the Modulation transfer function, MTF. The MTF, shown in Figure 2, conveys the available system contrast as a function of spatial frequency in cycles/mm.

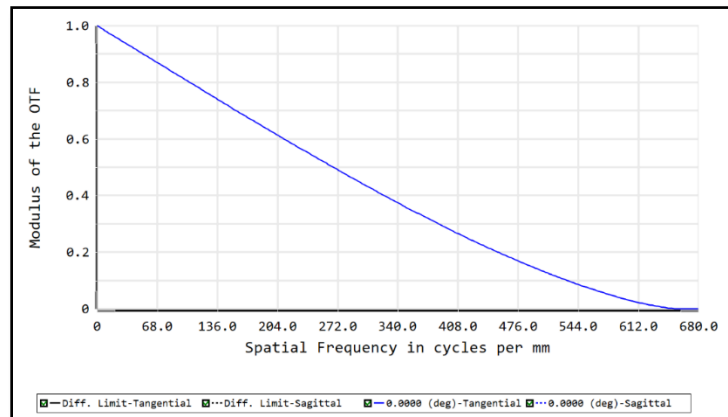


Figure 2: MTF Plot of a Diffraction Limited System:  $F/1.48$  at  $1 \mu\text{m}$

In the real world, nothing is ideal. Aberration present on the mirrors or lens of the telescope would change the transfer function and impulse response. As a result, the PSF would lose its central lobe peak and the cut off MTF performance curve will shift left to lower resolution values.

## 1.2 Wavefront Aberrations

Wavefront errors are measured against a reference, usually a flat wavefront. There are two metrics to summarize the errors: Peak-to-Valley and RMS wavefront error. Peak-to-Valley value (P-V) is the sum of the peak and trough values found in the span of the wavefront. This often would give the worst-case error because the errors could be from an outlier point in a localized region. The RMS wavefront error takes the root-mean-square of all the errors across the wavefront. This offers a more realistic overall error since it would alleviate the effects of a localized peak to valley error. P-V and RMS error are general parameters to quantify wavefront errors. To identify what errors attribute to the deformities, an erroneous wavefront's shape needs to be decomposed into identifiable quantity and quality. One way of describing the shape is to use Zernike polynomial fittings. These polynomials decompose the wavefront into types of known aberrations as well as the magnitude of the aberrations. One important reason why Zernike polynomials work is because they are orthogonal over the circular aperture, meaning there is no cross talk between each Zernike term or types of aberration.

Zernike polynomials define wavefront deviations as a function of a normalized pupil coordinate and a normalized object height,  $h$ . Figure 3 shows the normalized pupil coordinate is composed of radial distance on a pupil plane,  $\rho$ , and angular circular component,  $\theta$ .

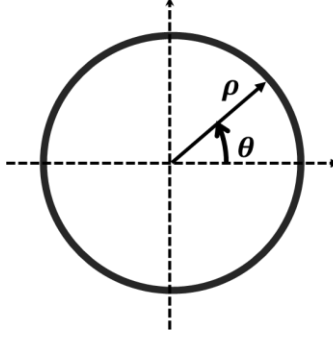


Figure 3: The normalized pupil coordinate is composed of radial distance on a pupil plane,  $\rho$ , and angular circular component,  $\theta$ .

There are various types of Zernike ordering. We will be using the same ordering as by Noll (5).

$$Z_j(\rho, \theta) \equiv Z_n^m(\rho, \theta) = \sqrt{\frac{2(n+1)}{1+\delta_{m0}}} R_n^m(\rho) \begin{cases} \cos m\theta \\ \sin m\theta \end{cases} \quad [20]$$

Where  $j$  = polynomial ordering number and is a function of

$n$  = radial degree and azimuthal frequency  $m$ ,

$\delta_{m0}$  = Kronecker Delta  $\delta_{m0} = 1$  for  $m = 0$ ,  $\delta_{m0} = 0$  for  $m \neq 0$

All  $n$  and  $m$  are positive integers where the quantity,  $n-m$ , is greater than or equal to 0 and is also

even.  $R_n^m(\rho)$  is a polynomial of degree  $n$  in  $\rho$ .

$$R_n^m(\rho) = \sum_{s=0}^{(n-m)/2} \frac{(-1)^s (n-s)!}{s! \left(\frac{n+m}{2}-s\right)! \left(\frac{n-m}{2}-s\right)!} \rho^{n-2s} \quad [21]$$

$R_n^m(\rho)$  is the radial circle polynomial, varying with  $\rho$

Each Zernike polynomial has both  $\cos m\theta$  and  $\sin m\theta$  components. Polynomial are ordered with an even  $j$  corresponding to a symmetric polynomial varying as a function of  $\cos m\theta$ . Odd values of  $j$  would correspond to antisymmetric polynomial, varying with  $\sin m\theta$ . Within each  $n$ th order sets, there will be multiple  $m^{\text{th}}$  values.

<b>First Order Aberration Only</b>				
<b>j</b>	<b>n</b>	<b>m</b>	<b><math>Z_j(\rho, \theta)</math></b>	<b>Aberration Name</b>
1	0	0	1	Piston
2	1	1	$2\rho \cos \theta$	X Tilt
3	1	1	$2\rho \sin \theta$	Y Tilt
<b>Second Order Aberration Only</b>				
<b>j</b>	<b>n</b>	<b>m</b>	<b><math>Z_j(\rho, \theta)</math></b>	<b>Aberration Name</b>
4	2	0	$\sqrt{3} (2\rho^2 - 1)$	Defocus
5	2	2	$\sqrt{6} \rho^2 \sin 2\theta$	Primary Astigmatism at 45°
6	2	2	$\sqrt{6} \rho^2 \cos 2\theta$	Primary Astigmatism at 0°
<b>Third Order Aberration Only</b>				
<b>j</b>	<b>n</b>	<b>m</b>	<b><math>Z_j(\rho, \theta)</math></b>	<b>Aberration Name</b>
7	3	1	$\sqrt{8} (3\rho^3 - 2\rho) \sin \theta$	Vertical Coma
8	3	1	$\sqrt{8} (3\rho^3 - 2\rho) \cos \theta$	Horizontal Coma
9	3	3	$\sqrt{8} \rho^3 \sin 3\theta$	Trefoil at 0°
10	3	3	$\sqrt{8} \rho^3 \cos 3\theta$	Trefoil at 45°
<b>Fourth Order Aberration Only</b>				
<b>j</b>	<b>n</b>	<b>m</b>	<b><math>Z_j(\rho, \theta)</math></b>	<b>Aberration Name</b>
11	4	0	$\sqrt{5} (6\rho^4 - 6\rho^2 + 1)$	Primary Spherical
12	4	2	$\sqrt{10} (4\rho^4 - 3\rho^2) \cos 2\theta$	Secondary Astigmatism at 0°
13	4	2	$\sqrt{10} (4\rho^4 - 3\rho^2) \sin 2\theta$	Secondary Astigmatism at 45°
14	4	4	$\sqrt{10} 4\rho^4 \cos 4\theta$	Quadrafoil in at 0°
15	4	5	$\sqrt{10} 4\rho^4 \sin 4\theta$	Quadrafoil in at 45°
<b>Fifth Order Aberration Only</b>				
<b>j</b>	<b>n</b>	<b>m</b>	<b><math>Z_j(\rho, \theta)</math></b>	<b>Aberration Name</b>
16	5	1	$\sqrt{12} (10\rho^5 - 12\rho^3 + 3\rho) \cos \theta$	Secondary x coma
17	5	1	$\sqrt{12} (10\rho^5 - 12\rho^3 + 3\rho) \sin \theta$	Secondary y coma
18	5	3	$\sqrt{12} (5\rho^5 - 4\rho^3) \cos 3\theta$	Secondary Trefoil at 45°
19	5	3	$\sqrt{12} (5\rho^5 - 4\rho^3) \sin 3\theta$	Secondary Trefoil at 0°
20	5	5	$\sqrt{12} \rho^5 \cos 5\theta$	Pentafoil at 45°
21	5	5	$\sqrt{12} \rho^5 \sin 5\theta$	Pentafoil at 0°

Table 1: All different orders of Zernike's expression and corresponding aberration name. (5)

The total aberration is the sum of the individual Zernike modes and their corresponding weights for a given system, according to equation [22]

$$\Phi(\rho, \theta) = \sum_{n=0}^{\infty} \sum_{m=0}^n C_{nm} Z_n^m(\rho, \theta) \quad [22]$$

Where  $\Phi(\rho, \theta)$  is the aberration function,  
 $C_{nm}$  is the Zernike expansion coefficient,  
and  $Z_n^m(\rho, \theta)$  is the specific polynomial.

From Table 1, Fourth Order Zernike Errors include polynomial errors in  $n=4$ . This includes  $j=11$ : Primary Spherical Aberration,  $j=12, 13$ : Secondary Astigmatism at 0 and 45 degrees, and  $j=14,15$ : Quadrafoil in Vertical and Oblique. Fifth Order Zernike Errors include all errors in  $n=5$ . This includes  $j=16,17$ : Secondary Coma x and y,  $j=18, 19$ : Secondary Trefoil Oblique and Vertical, and  $j=20,21$ : Pentafoil Oblique and Vertical. Fourth and Fifth Order Zernike Errors would include all the errors in both  $n=4$  and  $n=5$ . The only aberrations will be used in this simulation are 2<sup>nd</sup> to 5<sup>th</sup> order Zernike Orders. The first order does not affect rms wavefront error.

With contribution from known aberration types, the RMS wavefront of the optical system can be then calculated using the expansion coefficient.

$$\sigma = \sqrt{\sum_{n=0}^{\infty} \sum_{m=0}^n C_{nm}^2} \quad [23]$$

An important limitation of the Zernike expansion is its restriction to circular apertures. Expansion polynomials for other geometries exist, see reference (5) and (6) for details.

### 1.3 Encircled and Ensquared Energy General Application

Encircled energy is defined as the total radiometric power in the specified geometry on a target or an image plane. The typical geometries used are circles and squares. The specified shape or size can be arbitrarily chosen depending on the application.

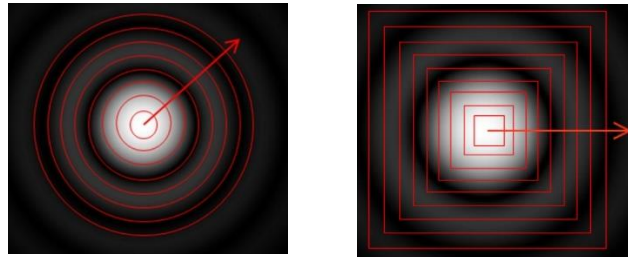


*Figure 4 :Inscribe energy region centered on the PSF. Left Encircled. Right Ensquared. [3]*

Encircled energy is used by astronomers to quantify instrument performance. However, the encircled energy is specified in object space angles rather than spatial size in image space. Often, an increment factor of the theoretical angular resolution,  $\frac{\lambda}{D}$ , is plotted against desired parameters of encircled energy. The optical system is then designed to meet these requirements. For a good imaging system, the design specifications would be tied to the behavior of a diffraction limited system where 84% of energy falls within the first central lobe.

A second common application of encircled energy is in laser acquisition systems. An optical system is designed to resolve a laser-illuminated distant target. Depending on where the PSF is located on the detector, one can locate the target by calculating the subtended angle between the target and the sensor.

Ensquared energy, with a square geometry, is often used in commercial camera applications. The majority of CCD and COMS detectors have square pixels, so it is easier to define the square region of interest by using number of pixels.

### 1.3.1 Encircled and Encircled Measurement Methods

Measuring encircled or ensquared energy can be very straight forward. The setup is illustrated in Figure 5.

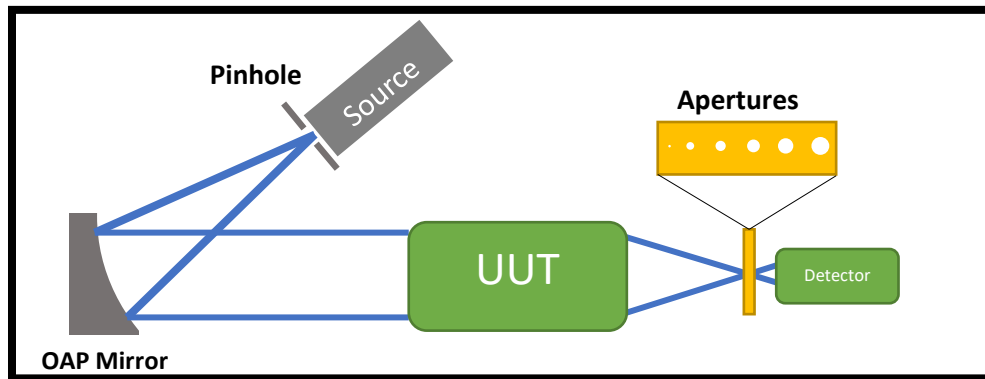


*Figure 5 Test Bench to measure Encircled Energy.*

The unit under test, UUT, is illuminated with a source of known wavelength. In Figure 5, the pinhole will be served as the object the UUT would image. Depending on how the UUT is used for imaging, it would either need to be placed at a finite imaging conjugate distance from the pinhole or placed at a location where the pinhole is collimated. For an infinite conjugate configuration, the pinhole would be placed 1 focal length away from a collimating optic. In Figure 5, the collimating optic would be the Off-Axis Parabola (OAP). At the image plane of the UUT, a series of apertures with known sizes are placed there. The aperture would be circular for Encircled Energy measurement or square for Ensquared measurement. One would record the power reading with a photodiode and associate it with the aperture size for data collection.

The mask size tolerance is important. A HeNe system, a relatively short wavelength at 0.633um paired with a F/1.4 optical system, produces an airy pattern diameter of only 2 um. Any meaningful tolerance on the pinhole needs to be less than 2 um; the usual rule of thumb suggests 10% of 2 um depending on the needed accuracy of the measurement. Recent advances in micromachining in a thin silicon substrate allow submicron precision (7).

Besides pinhole size accuracy, another method to refine measurement is to fine tune the location of the mask location at the focus. An additional lens can reimage the image plane of the UUT with magnification. The image of the mask and the PSF can then be viewed together as feedback for fine alignment.

Figure 5 illustrates the test bench which could be used for on and off axis field testing of the UUT. The pinhole location relative to the optical axis of the OAP Collimating Mirror can be translated to simulate an off-axis field, as shown below:

$$\theta_{off\ axis} = \text{atan} \left( \frac{\text{Pinhole Displacement}}{\text{Focal Length}_{OAP}} \right) \quad [24]$$

Figure 6 below shows the PSF and its cross-section of a simulated a F/1.4 system at 1 um wavelength.

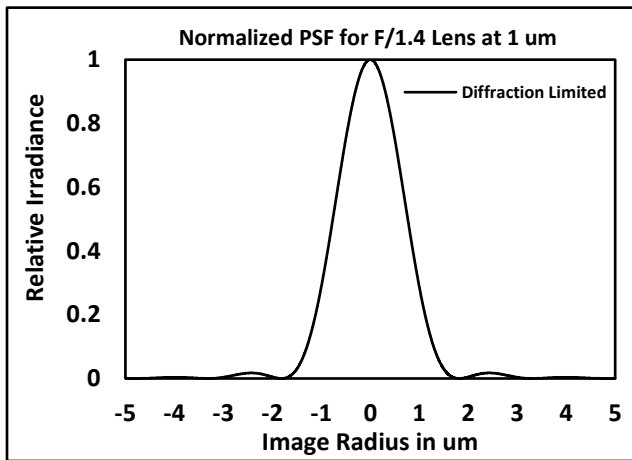


Figure 6

Figure 6: Cross section of the Point Spread Function of a F/1.4 system at 1 um in color scale.

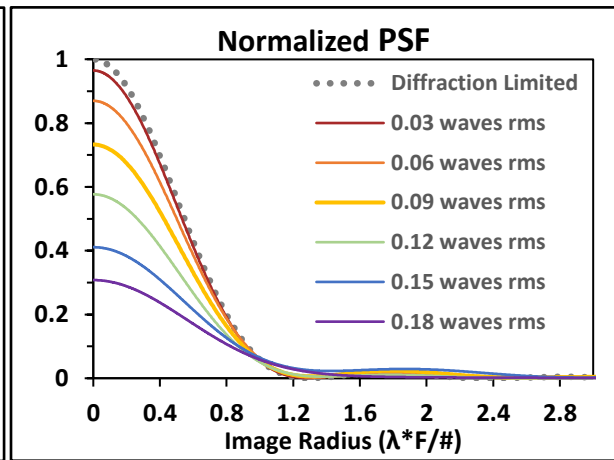


Figure 7

Figure 7: Cross section of the PSF with various rms wavefront error.

Figure 7 is an example of aberrated PSF with incrementing rms wave error. At 0.18 waves rms, the purple central lobe lost most of its intensity.

When collecting power from a diffraction limited PSF in Figure 6, the expected measured fractional encircled energy should follow the trend described in Figure 8 below. The first central lobe, in blue, stops at 1.7  $\mu\text{m}$ . The encircled energy corresponding to 1.7  $\mu\text{m}$  radius, in red, is 0.836 or 83.6% , the ensquared energy with 1.7  $\mu\text{m}$  half width, in green, is 0.84 or 84%.

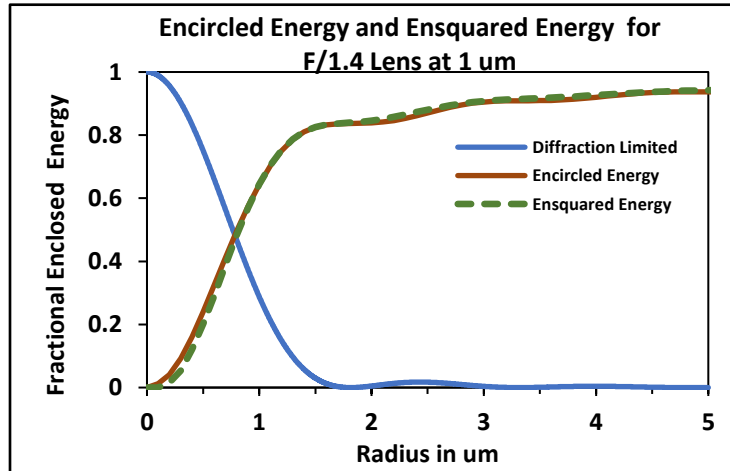


Figure 8 : Fractional inscribe energy of a diffraction limited F/1.4 system at 1  $\mu\text{m}$ . Ensquared Energy curve is slightly higher than the Encircled energy because circle is inscribed within the square of the same width. More area per the same width dimension.

### 1.3.2 Encircled and Ensquared Energy Analytical Solution Comparison

For a diffraction limited optical system with an unobscured circular pupil, the following equations could be used to calculate encircled and ensquared energy. The following equations are taken from Anderson (1) published from Applied Optics. The three parameters needed for calculation are the F-number, operational wavelength and the radius or half width of the encircled or ensquared area of interest. Equation (25) convert that physical dimension into a unitless radial value,  $p$ , shown in Figure 9.

$$p = \frac{s_1 \pi}{\lambda f/\#} \quad [25]$$

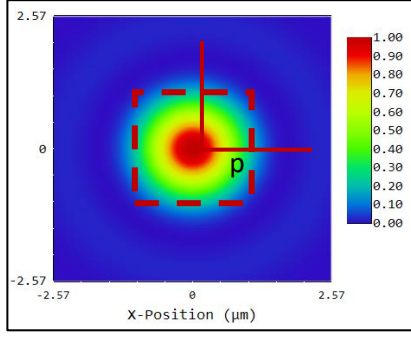


Figure 9 Radial distance of Ensquared Energy,  $p$ .

The double integral is shown in Equation (26) and Equation (27) further simplifies it to the difference between the Bessel Function of the 0<sup>th</sup> order and 1<sup>st</sup> order.

$$E_c(p) = \frac{1}{4\pi} \int_0^p \int_0^{2\pi} \left( \frac{2J_1(r)}{r} \right)^2 r d\theta dr \quad [26]$$

$$= 1 - J_0(p)^2 - J_1(p)^2 \quad [27]$$

This is an expression first derived by Lord Rayleigh (3). The Ensquared energy,  $E_s$ , can be calculated by the modification of the Encircled Energy calculation with the same radial distance.

$$E_s(p) = \frac{4}{\pi} \int_0^{\pi/4} E_c\left(\frac{p}{\cos\theta}\right) d\theta \quad [28]$$

The relationship between Encircled and Ensquared energy of the same half width can be described by the following inequality per Andersen's paper on inscribe energy calculation (3):

$$E_c(p) < E_s(p) < E_c(p\sqrt{2}) \quad [29]$$

For the same radius,  $p$ , there will be less energy in the encircled energy than in ensquared energy.

The analytical solution works well at 0 rms wavefront error and will be used as a baseline in optical simulation later.

An additional side note, if the input source is a single mode laser, an alternative encircled energy equation for Gaussian beam is needed. This is because the beam intensity is no longer a Bessel function but rather a Gaussian. The equation for the power transmission through an aperture for a Gaussian is derived in Siegman's book (10).

$$\text{Encircled Energy} = 1 - e^{-\frac{2a^2}{\omega^2}} \quad [27-b]$$

The encircled radius is  $a$  and the beam waist radius is  $\omega$ . An aperture radius with the same size as the waist radius will yield about 86% of the total power.

## Section 2: Simulation

### 2.1 Simulation Scope and Parameters

For an aberrated optical system, the different wavefront error types have different impact on the encircled energy value. Each type of aberration stretches the PSF uniquely. For example, 3<sup>rd</sup> order spherical creates a symmetric blur while 3<sup>rd</sup> order coma creates a tear shaped blur. Even though there is a mathematical correlation between Zernike coefficient to rms wavefront error, there isn't one for ensquared or encircled energy. This scope of the project is to simulate an ideal lens with wavefront perturbations. We generate individual errors using 2<sup>nd</sup>, 3<sup>rd</sup>, 4<sup>th</sup>, and 5<sup>th</sup> order Zernike modes, as well as errors from combined 4<sup>th</sup> and 5<sup>th</sup> modes. Finally, all modes from 2<sup>nd</sup> to 5<sup>th</sup> are considered in combination. For each Zernike order category, the simulation would randomize Zernike coefficients while yielding the targeted overall rms wavefront error. This is made possible using Equation 23, a property of the Zernike Coefficient to rms wavefront error. Monte Carlo methods are utilized to produce the same rms wavefront error results over many different unique Zernike coefficients combination. At the end of each run, the average ensquared and encircled energy radius is recorded, and fitting is performed for each rms wavefront error value.

The encircled and ensquared energy radius in  $\mu\text{m}$  would be recorded at two separate energy level: 85% & 95%. The wavefront errors are from 0 waves to 0.18 waves, in 6 steps with 0.03 waves increments. The optical systems simulated are F/1.4 with wavelengths 0.633  $\mu\text{m}$ , 1  $\mu\text{m}$ , and 3.39  $\mu\text{m}$ , and F/4, F/6 and F/8 at 1  $\mu\text{m}$  wavelength.

## 2.2 Monte Carlo Zemax Set Up

	Surface Type	ment	Radius	Thickness	Material	Maximum Term #	Norm Radius	Zernike 1	Zernike 2	Zernike 3	Zernike 4
0	OBJECT	Standard ▾	Infinity	Infinity							
1	(aper)	Standard ▾	Infinity	0.000...	2.00.0.0 M						
2	Zernike Standard Sag ▾		Infinity	0.000...		12	5.000000000...	0.000000000...	0.000000000...	0.000000000...	0.000000000...
3	STOP	Paraxial ▾		14.00...							
4		Standard ▾	Infinity	0.000...							
5	IMAGE	Standard ▾	Infinity	-							

Figure 10 Simulation Zemax Lens Data Manager

An excerpt from Zemax simulation is shown in Figure 10. Surface 2 has a Zernike Standard Sag surface type which is used to simulate aberrations. The surface type allows customization of additional of Zernike coefficient terms to tune surface deformities. A perfect infinite conjugate paraxial lens is used to focus the deformed wavefront. A macro then generates randomized Zernike coefficient inputs, while maintaining the targeted wavefront error at the focus. For each randomized Zernike coefficients set, the specified encircled and ensquared energy radius size is collected and averaged at the end.

To find the number unique of times Zernike coefficients are generated, three sample sizes were used as comparison. The three sample sizes were 100, 500 and 1000, The optical system used was a F/1.4 at 1 um wavelength with 4<sup>th</sup> order Zernike errors evaluating 95% Encircled Energy radius. The variability between 500 Samples and 1000 Samples encircled diameter sizes was less than 0.5% shown in Table 2; results converge within ~1 um. Due to reasonable calculation time and acceptable precision, 500 n-sample was chosen.

1 $\mu\text{m}$ , 4 <sup>th</sup> Order Zernike Error Only; 95% Encircled Energy			
Average Wavefront [waves]	<b>500 Samples</b> Average Encircled Energy Radius Value [ $\mu\text{m}$ ]	<b>100 Samples</b> Average % Deviation from 500 Samples	<b>1000 Samples</b> Average % Deviation from 500 Samples
0	5.84	-	-
0.03	6.20	0.09%	-0.20%
0.06	7.02	-0.01%	-0.01%
0.09	8.04	0.22%	0.02%
0.12	9.09	0.16%	0.13%
0.15	10.32	0.46%	-0.23%
0.18	11.55	-0.52%	-0.36%

Table 2: Three different sample sizes were analyzed for each targeted wavefront error.

The encircled and ensquared energy was calculated using the Optimization operand, DENC, Diffraction Encircled energy for distance. The baseline of pupil sampling was a grid of 256 X 256.

The Zemax macro is included in Appendix 1.

### Section 3: Results

For each optical parameter cases mentioned in Section 2.2, the macro used in Zemax simulation generated tables similar to the one in Figure 11. The results were recorded in an excel file for data processing.

Average Wavefront [wv]	RMS Average Ensquared [um]
0.0000	6.0712
0.0300	6.7000
0.0600	8.0089
0.0900	9.6805
0.1200	12.6102
0.1500	14.9594
0.1800	18.1449

Figure 11: Example Output File of Zemax Simulation

The raw data was fitted to an exponential curve to link rms wavefront error to averaged encircled or ensquared radius. The y intercept or the coefficients will be the radius value at 0 rms wavefront error value. The data could be fitted both quadratically or exponentially. An exponential relationship was chosen because of the more simplified form, and it would match an existing related relationship described in Equation 30. From Modern Optical Engineer book by Warren Smith (11), the Strehl Ratio degrades exponentially as rms wavefront error,  $\omega$  .

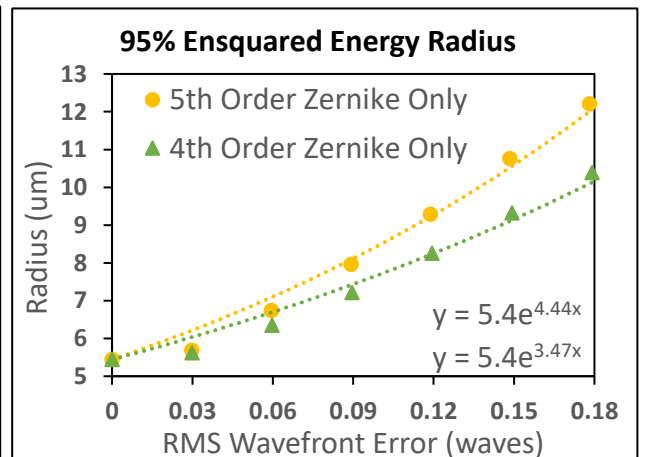
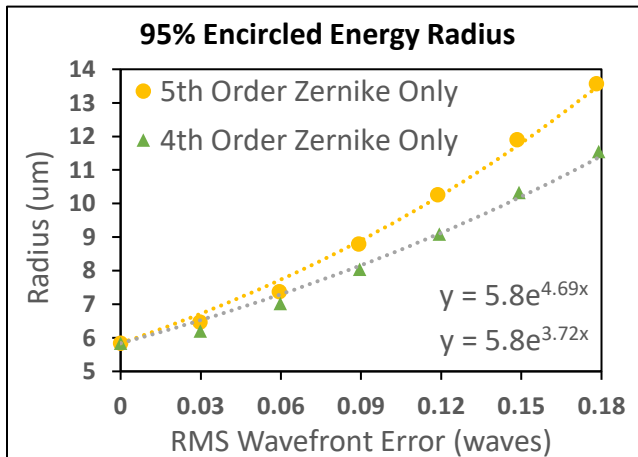
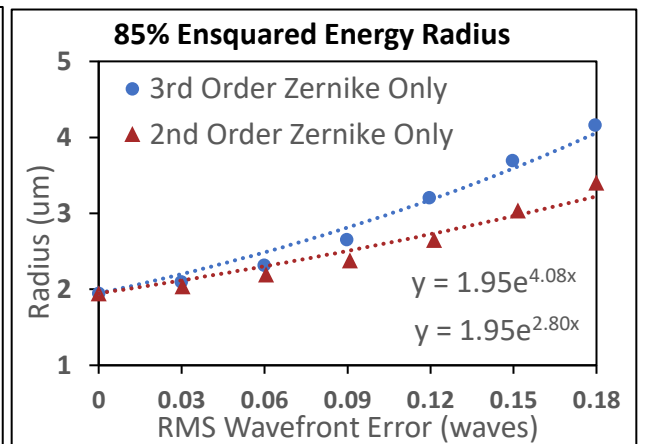
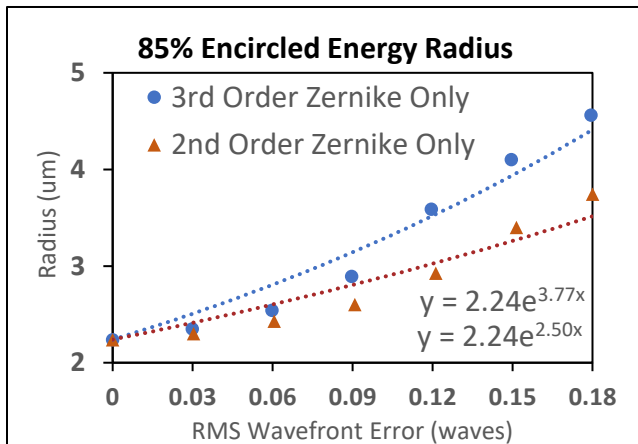
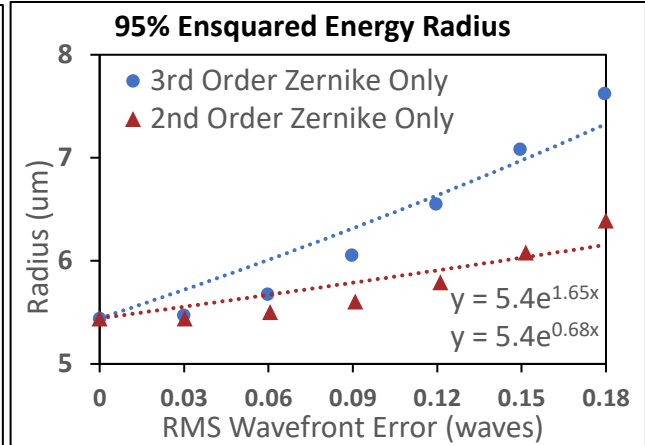
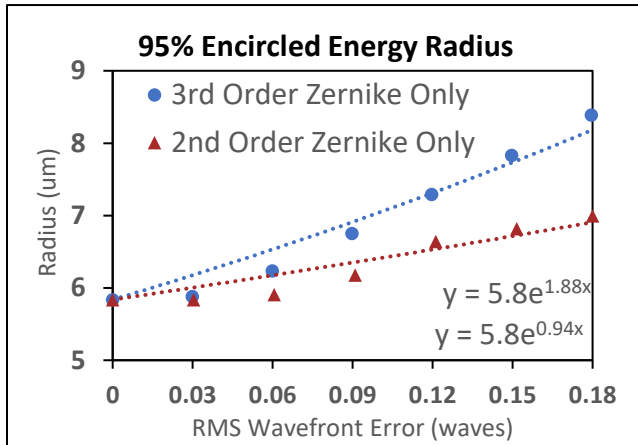
$$\text{Strehl Ratio} = e^{-(2\pi\omega)^2} \tag{30}$$

The Strehl Ratio is the ratio of the PSF central peak illumination of an aberrated system to a diffraction limited system. An optical system with aberrations will lose light in the central peak exponentially and redistribute the light to the outer regions. Therefore, an assumption was made that the encircled energy radius would also grow exponentially with wavefront error.

### 3.1 Plots of Raw data

#### 3.1.1 Zernike

At 1  $\mu\text{m}$  and F/1.48: 2<sup>nd</sup>, 3<sup>rd</sup>, 4<sup>th</sup>, 5<sup>th</sup>, 4<sup>th</sup> + 5<sup>th</sup>, and all orders (2<sup>nd</sup> to 5<sup>th</sup>) Zernike



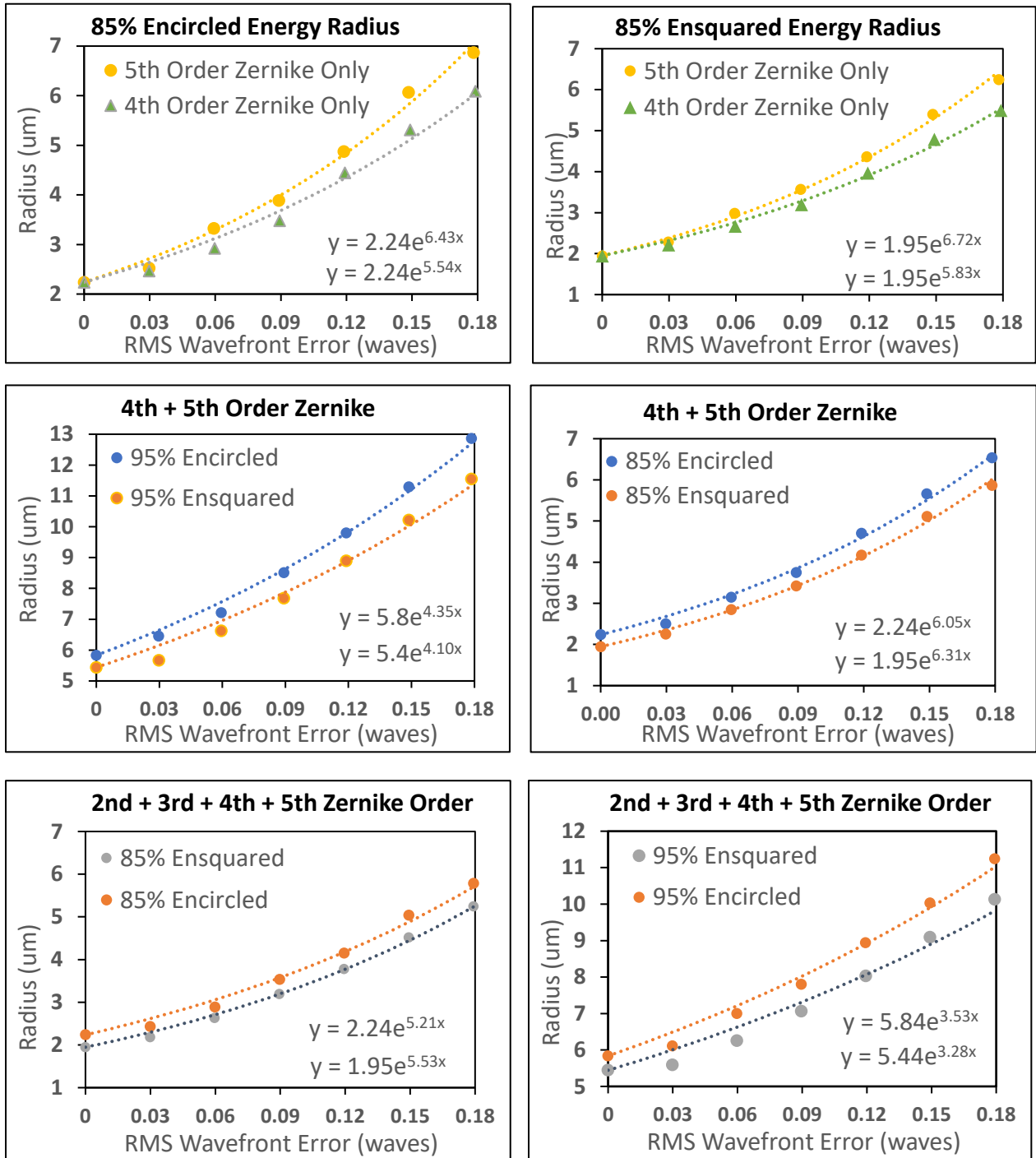


Figure 12: Zernike Order: 4th,5th, 4th + 5<sup>th</sup> and All Order (2<sup>nd</sup> to 5<sup>th</sup> Order) WFE vs Encircled and Ensquared Energy Radius.

### 3.2.2 F-Number

At 1um, 85% Encircled and Ensquared Energy and 5th Order Zernike Only: F/4, F/6, F8

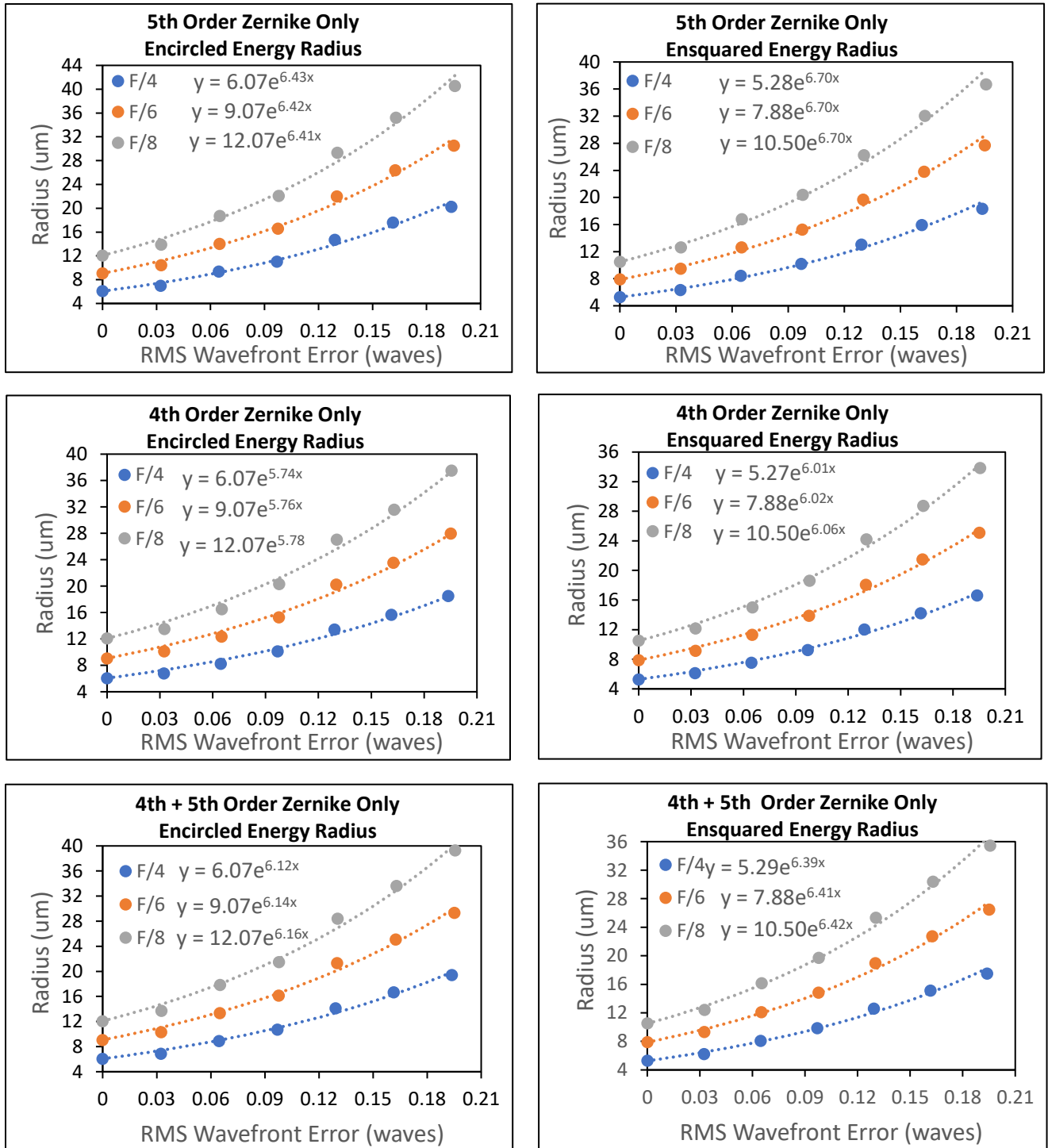


Figure 13 F-number with Zernike WFE vs Encircled and Ensquared Energy Radius.

### 3.2.3 Wavelength

At F/1.48, 85% Encircled and Ensquared Energy and 5<sup>th</sup> Order Zernike Only: Lambda=0.633 um ,3.99um

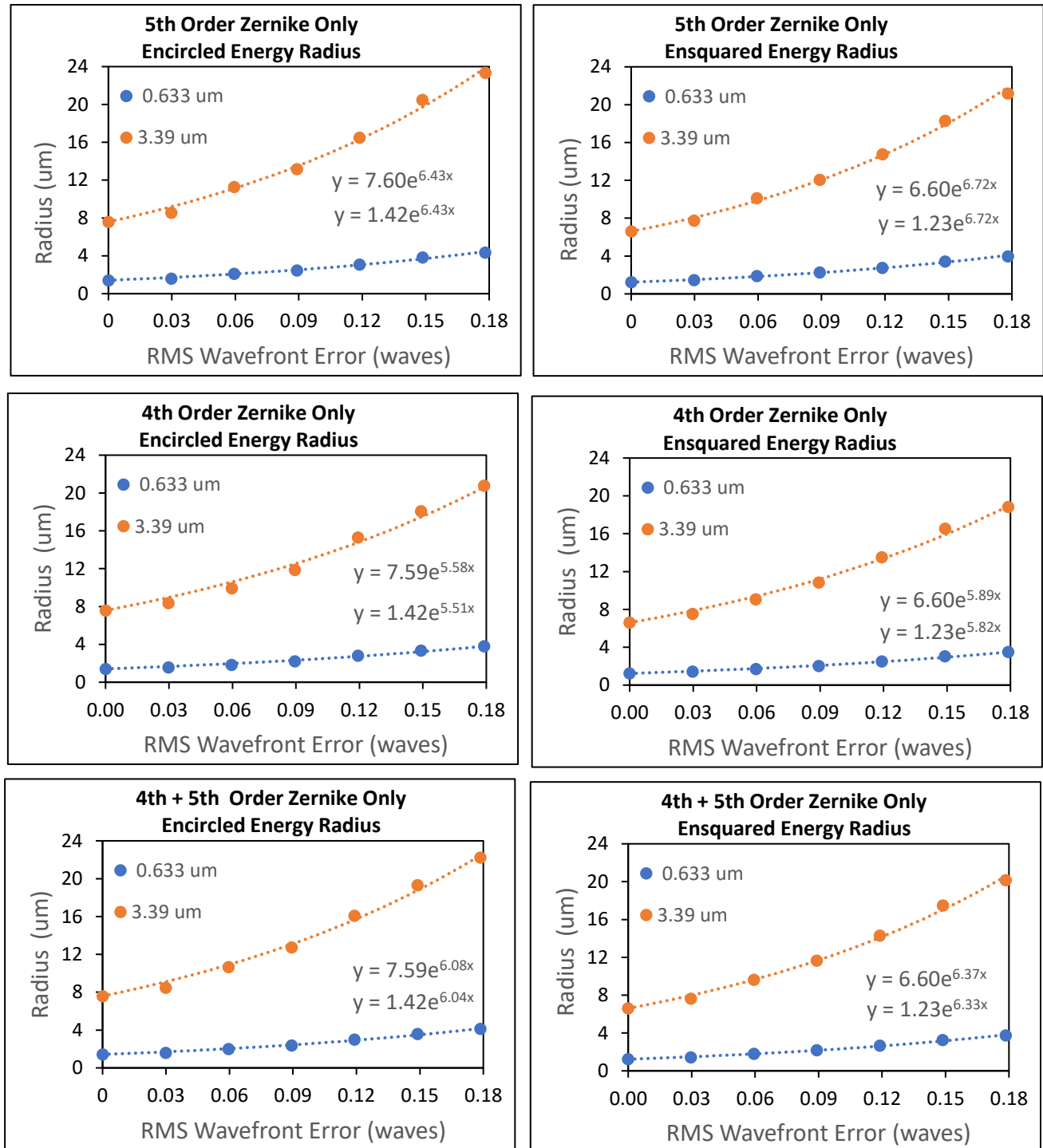


Figure 14 Wavelength with Zernike WFE vs Encircled and Ensquared Energy Radius.

## 3.2 Fitted Equations

The results from the Monte Carlo runs are fitted into equations below.

With Second Order Zernike Aberration

$$85\% \text{ Encircled Energy Radius} = 1.50 \lambda f/\# e^{\frac{2.50 wfe}{\lambda}} \quad [31]$$

$$85\% \text{ Ensquared Energy Radius} = 1.31 \lambda f/\# e^{\frac{2.80 wfe}{\lambda}} \quad [32]$$

$$95\% \text{ Encircled Energy Radius} = 3.92 \lambda f/\# e^{\frac{0.94 wfe}{\lambda}} \quad [33]$$

$$95\% \text{ Ensquared Energy Radius} = 3.65 \lambda f/\# e^{\frac{0.68 wfe}{\lambda}} \quad [34]$$

With Third Order Zernike Aberration

$$85\% \text{ Encircled Energy Radius} = 1.50 \lambda f/\# e^{\frac{3.77 wfe}{\lambda}} \quad [35]$$

$$85\% \text{ Ensquared Energy Radius} = 1.31 \lambda f/\# e^{\frac{4.08 wfe}{\lambda}} \quad [36]$$

$$95\% \text{ Encircled Energy Radius} = 3.92 \lambda f/\# e^{\frac{1.88 wfe}{\lambda}} \quad [37]$$

$$95\% \text{ Ensquared Energy Radius} = 3.65 \lambda f/\# e^{\frac{1.65 wfe}{\lambda}} \quad [38]$$

With Fourth Order Zernike Aberration

$$85\% \text{ Encircled Energy Radius} = 1.50 \lambda f/\# e^{\frac{5.76 wfe}{\lambda}} \quad [39]$$

$$85\% \text{ Ensquared Energy Radius} = 1.31 \lambda f/\# e^{\frac{6.03 wfe}{\lambda}} \quad [40]$$

$$95\% \text{ Encircled Energy Radius} = 3.92 \lambda f/\# e^{\frac{3.72 wfe}{\lambda}} \quad [41]$$

$$95\% \text{ Ensquared Energy Radius} = 3.65 \lambda f/\# e^{\frac{3.47 wfe}{\lambda}} \quad [42]$$

With Fifth Order Zernike Aberration

$$85\% \text{ Encircled Energy Radius} = 1.50 \lambda f/\# e^{\frac{6.43 wfe}{\lambda}} \quad [43]$$

$$85\% \text{ Ensquared Energy Radius} = 1.31 \lambda f/\# e^{\frac{6.70 wfe}{\lambda}} \quad [44]$$

$$95\% \text{ Encircled Energy Radius} = 3.92 \lambda f/\# e^{\frac{4.7 wfe}{\lambda}} \quad [45]$$

$$95\% \text{ Ensquared Energy Radius} = 3.65 \lambda f/\# e^{\frac{4.4 wfe}{\lambda}} \quad [46]$$

With Fourth and Fifth Order Zernike Aberration

$$85\% \text{ Encircled Energy Radius} = 1.50 \lambda f/\# e^{\frac{6.14 wfe}{\lambda}} \quad [47]$$

$$85\% \text{ Ensquared Energy Radius} = 1.31 \lambda f/\# e^{\frac{6.41 wfe}{\lambda}} \quad [48]$$

$$95\% \text{ Encircled Energy Radius} = 3.92 \lambda f/\# e^{\frac{4.35 wfe}{\lambda}} \quad [49]$$

$$95\% \text{ Ensquared Energy Radius} = 3.65 \lambda f/\# e^{\frac{4.10 wfe}{\lambda}} \quad [50]$$

With all Aberrations Case:

$$85\% \text{ Encircled Energy Radius} = 1.50 \lambda f/\# e^{\frac{5.21 wfe}{\lambda}} \quad [51]$$

$$85\% \text{ Ensquared Energy Radius} = 1.31 \lambda f/\# e^{\frac{5.53 wfe}{\lambda}} \quad [52]$$

$$83.8\% \text{ Encircled Energy Radius} = 1.22 \lambda f/\# e^{\frac{2\pi wfe}{\lambda}} \quad [53]$$

The unit of wfe is in waves. Example values calculated from Equation 51 and Equation 52 using a F/1.49 system at 1  $\mu\text{m}$  are listed in Table 3.

F/1.49, Wavelength = 1 $\mu\text{m}$	
RMS Wavefront Error (wave)	85% Encircled Energy Radius [ $\mu\text{m}$ ]
0.00	2.24
0.03	2.62
0.06	3.06
0.09	3.57
0.12	4.17
0.15	4.88
0.18	5.70

F/1.49, Wavelength = 1 $\mu\text{m}$	
RMS Wavefront Error (wave)	85% Ensquared Energy Radius [ $\mu\text{m}$ ]
0.00	1.95
0.03	2.30
0.06	2.71
0.09	3.20
0.12	3.78
0.15	4.45
0.18	5.26

Table 3: 85% Encircled and Ensquared energy radius calculated for 2<sup>nd</sup> to 5<sup>th</sup> Order Zernike Errors using Equation 51 and 52.

Example values calculated from Equation 53 using a F/5 system at 1  $\mu\text{m}$  are listed in Table 4.

F/5, Wavelength = 1 $\mu\text{m}$	
RMS Wavefront Error (wave)	83.8% Encircled Energy Radius ( $\mu\text{m}$ )
0.00	6.10
0.03	7.48
0.06	9.17
0.09	11.25
0.12	13.79
0.15	16.91
0.18	20.73

Table 4: 83.8% Encircled Energy radius calculated for 2<sup>nd</sup> to 5<sup>th</sup> Order Zernike Errors using Equation 53

## Section 4: Discussion

$$85\% \text{ Encircled Energy Radius} = \underbrace{1.50}_{\text{Coefficient}} \lambda f/\# e^{\overbrace{6.43 wfe}^{\text{Exponential}}} \quad [43]$$

Coefficient Comparison with Monte Carlo and Analytical Solution for Diffraction Limited Case				
Fractional Energy		Analytical Solution	Monte Carlo	Percent Difference (%)
85%	Ensquared	1.30	1.31	0.8
	Encircled	1.50	1.50	0.0
95%	Ensquared	3.64	3.65	0.3
	Encircled	3.92	3.92	0.0

Table 5: Comparison of Analytical Solution vs Monte Carlo Results from 85% and 85% Inscribe Energy.

To anchor the Monte Carlo results, the coefficients from the fitted equation was first compared to the analytical solution. The analytical method would only work with 0 wavefront error. Therefore, the exponential term is eliminated in the Monte Carlo equations. The analytical solution for the coefficient was calculated using the Matlab code attached in Appendix 1. The coefficients of the Encircled Energy are identical shown in Table 5. The Ensquared Energy coefficient is almost identical, with less than a percent difference. This might be due to a minor sampling method difference in the Zemax calculation and the analytical method. The wavelengths and f-number are built into the coefficient term because the ideal PSF should scale with wavelengths and f-number, as shown in Equation [19]. Therefore, this will also be reflected in the encircled and ensquared energy radius calculation as coefficients.

Next, the exponential term determines how fast the encircled and ensquared energy radius grow as a function of wavefront error caused by various Zernike terms. The exponential term grows with increasing Zernike Order. This means for the same wavefront error, higher frequency ripples across the pupil will create a bigger focus spread. For design that uses encircled or ensquared energy metric, one would control the aberration to lower orders contribution.

There are minor differences with the fitted equation results and the raw data. From looking at the raw data plots in the previous section, not all dots overlapped with the trendline. The trendline for specific aberration case, Equation 31 to Equation 50, have a residual sum of squares, (RSS), error value of 3.82% compared to the raw data. The trendline does a better job fitting rms wavefront error from 0.09 waves to 0.18 waves, with peak error of 5%. For rms wavefront error from 0.03 waves to 0.06 waves, the peak error is 7%. This is due to the inflection point of the exponential curve, taking off slightly faster than the raw data.

For encircled energy case with all aberration case, Equation 51, the RSS error value is 4% compared to raw data. The peak encircled energy radius error is 8% error at 0.03 waves rms error. For ensquared energy case with all aberration case, Equation 52, the RSS error value 3% compared to raw data. The peak error is 6% evaluating at 0.03 waves rms error.

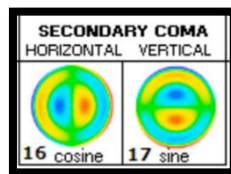


Figure 15: Secondary Coma (6)

The Monte Carlo simulation suggests that optical systems with higher order Zernike term wavefront errors will have a faster spot size growth with rms wavefront error than lower orders. This is shown with the smaller exponential term 4<sup>th</sup> order only Zernike has compared to 5<sup>th</sup> order only Zernike, across all evaluation parameters. This could be attributed to aberrations in 5<sup>th</sup> order Zernike set such as secondary coma. From Figure 15, secondary coma deforms the wavefront into 2 centered concentric lobes enclosed by a bold ring in the outer region. The asymmetrical wavefront error could be changing the impulse response such that more light is going to the outer region of the central focus point. For an optical system with 4<sup>th</sup> and 5<sup>th</sup> Zernike Wavefront error, the exponential term landed between those two cases. This trend indicates that when designing

optical system with emphasis on encircled and encircled energy performance, it is critical to control aberrations profile to lower Zernike orders.

In summary, the equations derived are tailored to specific Zernike aberration cases. Equation 51 and 52 are the most important relationship because including aberrations from 2<sup>nd</sup> to 5<sup>th</sup> order is the most realistic scenario. For a simplified takeaway, one additional equation was derived in the most generic format. Equation 53 approximates the encircled energy radius capturing the same total energy value found in the central lobe of a perfect psf, 83.8%, in an aberrated system.

$$83.8\% \text{ Encircled Energy Radius} = 1.22 \lambda f/\# e^{\frac{2\pi w f e}{\lambda}} \quad [53]$$

This equation works for wavefront error from 0 to 0.10 waves rms. The RSS error value compared to the raw data is 10% with peak error value of 14% at 0.10 waves rms.

## Section 5: Conclusion

A Monte Carlo analysis is performed to generate unique combinations of Zernike wavefront errors that yield the same overall rms error of the optical system. Zernike errors from orders 2<sup>nd</sup> through 5<sup>th</sup> are considered individually, as well as errors from 4<sup>th</sup> and 5<sup>th</sup> orders combined. Finally, all orders from 2<sup>nd</sup> to 5<sup>th</sup> are considered in combination. The results are generated with a Zemax model of an aberrated wavefront surface controlled by a macro and then focused with a perfect paraxial lens. The macro generated many independent randomized magnitudes values for Zernike terms and calculated the averaged Encircled or Ensquared Energy radius at 85% and 95% energy level at the end of 500 runs. The optical system simulated has an unobscured circular entrance pupil. In addition, the various parameters include f/1.4, f/4, f/6, and f/8 at operating wavelengths of 0.633 um, 1 um and 3.39 um.

We provided unique equations to approximate encircled and ensquared energy radius for each aberration case for wavefront error up to 0.18 waves rms. The mathematical relationship derived from the Monte Carlo runs were validated at zero wavefront error with existing analytical methods. The fitted equations from the Monte Carlo simulations have an RSS error of ~5% compared to the raw data.

One additional equation was derived to take on the most simplified format. This equation approximates 83.8% encircled energy radius for wavefront error up to 0.10 waves rms. It takes into consideration all Zernike orders from 2<sup>nd</sup> to 5<sup>th</sup> and overall has an RSS fitting error of 10%.

$$83.8\% \text{ Encircled Energy Radius} = 1.22 \lambda f/\# e^{\frac{2\pi wfe}{\lambda}}$$

These equations push past the conventional analytical solution limitations and lower calculation time. This method would be a great approximation tool in determining whether encircled or ensquared radius is achievable given a wavefront error requirement in the design planning phase.

# Appendix 1

## Zemax Macro

```
!Last Updated 6/4/2023 for Strehl
print "Average Wavefront [wv] RMS Average Ensquared [um]" " Average RMS Spot Diameter
[um] Average Strehl Ratio"
!Step through increment of rms values
!Number of loops
n=500
surp 2,10,0,13

!Start 0.05, End 2, Increment of 0.05
For r,0,0.09,0.09

!Chang sampling of ensquared energy merit function
if (r<0.6)
    setoperand 2,2,4
Endif
if (r>0.6)
    setoperand 2,2,5
endif

if (r>1.1)
    setoperand 2,2,6
endif

if (r>1.5)
    setoperand 2,2,7
endif

!Input RMS wave error target value
factor=r
!print "factor ",factor
zemax=1.09

!(Zernike 1_st order to _# order in (Z#)
zernterms1_1=3
zernterms1_2=6
zernterms1_3=10
zernterms1_4=15
zernterms1_5=21

!Picking (order n) 4th order zernikies

!(order n - order n-1)
delta1=zernterms1_4-zernterms1_3
zernterms=delta1
```

```

!"First" cut off all terms leading to 4th order, (order n-1)
first=zernterms1_3 + 1
second=zernterms1_4 -1

!print "num terms ",zernterms

!!!!!!!!!!!!!!!!!!!!!!!!!!!!!!!!!!!!!!!!!!!!!!!!!!!!!!!!!!!!!!!!!!!!!!!!!!!!
!Clear old terms and Assign Number of zernike terms to surface 2
surp 2,10,0,13
surp 2,10,first+delta1-1,13
!Factor to make math agree with zemax values
factor=factor*zemax
wave=WAVL(1)

!resetting sum calculation
yy=0
ww=0
rms2=0
str2=0

For k, 1, n , 1
zz=0
!13
!Random coefficients are written to the extra data editor for surface 2
for i, first+2, first+1+zernterms, 1
!factor are random value chosen
z=(rand(2)-1)/1
zz=zz+z*z
!11
surp 2, 11, z, i
!print "z ",z
next
zz=sqrt(zz)

! the coefficients by the rms
getextradata 1, 2
for i, first+2, first+1+zernterms, 1
x= factor*wave*vec1(i)/zz*0.001
surp 2, 11, x, i
!print "x ",x
next

update all

y=oper(1,10)
w=oper(2,10)
rms=oper(3,10)
str=oper(4,10)

!print y,w

```

```

yy=yy+y
ww=ww+w
rms2=rms2+rms
str2=str2+str
!print y, " ",w
next

!"Average Wavefront RMS ", "Average Ensquared", "Average RMS Spot Diameter so *2 and *1000 for
um"
print yy/n, " ", ww/n, " ",rms2/n*2*1000," ",str2/n
next

```

## Matlab Code

```

% Inscribe Energy Calculation for diffractive limited Bessel Function
% From Paper: Accurate calculation of diffraction-limited encircled and ensquared energy by TORBEN
B. ANDERSEN
% Wriiten By : Sze Wah Lee
% 6/25/2023

clc
clear

% User Input Lens Parameter
fno=1.48674;
lam=1; % 1 um

% User Input P (P is a unitless value in Bessel Function Coordinate
p=4.71; % For First Bessel Lobe % Es 85% =4.075/95% for 11.45

fun = @(p) 1-besselj(0,p).^2-besselj(1,p).^2;

% Percent Encircled Energy per p radius
Ec=fun(p)% Percent Energy
%
fun2=@(theta) fun(p./cos(theta));
% Percent Ensquared Energy per p radius
Es=4/pi*integral(fun2,0,pi/4)

% %
% Finding the radius per Fractional Encircled Energy
syms p theta
fno=1.48674; % F-number % User Input
lam=1; % Wavelength in um % User Input

percentage=0.85; % User Input
fun = 1-besselj(0,p).^2-besselj(1,p).^2==percentage;
enc_p=solve(fun)
coeff=double(enc_p)/pi % coefficient without the lambda*f-num
Physical_radial_dist=double(enc_p)/pi*fno*lam

```

## References

- (1) Clark, Peter P., et al. "Asymptotic Approximation to the Encircled Energy Function for Arbitrary Aperture Shapes." *Applied Optics*, vol. 23, no. 2, 15 Jan. 1984, pp. 353–357, <https://doi.org/10.1364/ao.23.000353>.
- (2) David Shafer, "Encircled Energy Performance Prediction Formula For Tolerancing," Proc. SPIE 0193, Optical Systems in Engineering I, (29 November 1979); doi: 10.1117/12.957870
- (3) Andersen, Torben B. "Accurate Calculation of Diffraction-Limited Encircled and Ensquared Energy." *Applied Optics*, vol. 54, no. 25, 2015, p. 7525, <https://doi.org/10.1364/ao.54.007525>.
- (4) Mahajan, Virendra; N. "Zernike Polynomials and Beyond 'Introduction to Aberrations.'" 7 July 2023, University of Arizona.
- (5) Noll, Robert. "Zernike Polynomials and Atmospheric Turbulence\*." *Journal of the Optical Society of America*, vol. 66, no. 3, 1976, p. 207, <https://doi.org/10.1364/josa.66.000207>.
- (6) Sacek, Vladimir. "3.5.3. Zernike Expansion Schemes." *Zernike Expansion Schemes*, [www.telescope-optics.net/zernike\\_expansion\\_schemes.htm](http://www.telescope-optics.net/zernike_expansion_schemes.htm). Accessed 25 June 2023.
- (7) Leviton , Douglas, and Sridhar M Manthripragada. "Method of Measuring Encircled Energy for Imaging Optics." *Tech Briefs*, 13 Sept. 2019, [www.techbriefs.com/component/content/article/tb/supplements/ptb/briefs/29551](http://www.techbriefs.com/component/content/article/tb/supplements/ptb/briefs/29551).
- (8) Surgent, Justin. "Encircled Energy and Ensquared Energy on LensCheck™ Lens Measurement Systems." *Optikos*, 4 May 2022, [www.optikos.com/articles/encircled-energy-and-ensquared-energy-on-lenscheck-lens-measurement-systems/](http://www.optikos.com/articles/encircled-energy-and-ensquared-energy-on-lenscheck-lens-measurement-systems/).
- (9) W. J. Smith, *Modern Optical Engineering*, 3rd ed. (McGraw-Hill, 2000), pp. 383–385.
- (10) Siegman, Anthony E. "Physical Properties of Gaussian Beams." *Lasers*, University of Science Books., Mill Valley, CA, 1986, pp. 664–667.
- (11) Smith, Warren J. *Modern Optical Engineering*, 4th ed., SPIE, New York, 2008, pp. 375–376.